

Development of a Robust Ring-Closing Metathesis Reaction in the Synthesis of SB-462795, a Cathepsin K Inhibitor

Huan Wang,^{*,†} Steven N. Goodman,[†] Qunying Dai,[†] Gregory W. Stockdale,[‡] and William M. Clark, Jr.[†]

Chemical Development and Statistical Sciences, GlaxoSmithKline, 709 Swedeland Road, King of Prussia, Pennsylvania 19406, U.S.A.

Abstract:

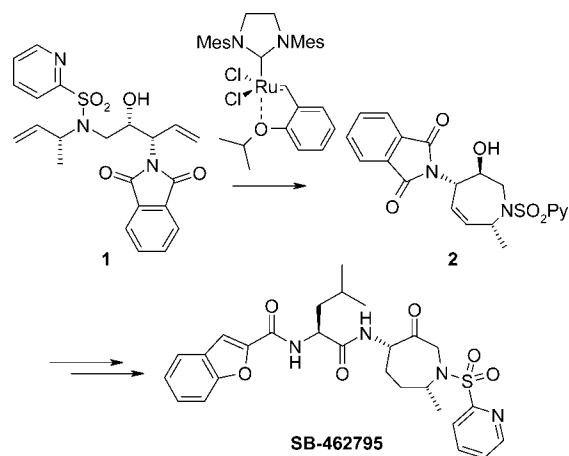
The development of a robust and high-yielding ring-closing metathesis (RCM) reaction and its demonstration on multikilogram scale are described. A detailed understanding of the impact of impurities on the RCM reaction was achieved using a variety of chemical and statistical methods. Specifically, individual impurities were evaluated in spiking studies to identify those that negatively affected the RCM reaction. Projection methods (PCA and PLS) were applied to historical data to identify the main sources of variation in starting material quality and determine the main detrimental impurities that impeded the RCM reaction. The synthesis of the starting material was then modified to adequately control these key impurities, which in turn ensured a robust RCM process. Finally, the robustness of the RCM reaction was assessed using a probability-based approach.

Introduction

During the past decade, the ring-closing metathesis (RCM) reaction has emerged as a powerful tool for C–C bond formation.¹ Not only has this methodology been widely used in academic research, but it has been extended to include large-scale synthesis in a pharmaceutical setting.² The sensitivity of the RCM reaction to impurities is a key challenge for developing a robust industrial process, since the efficiency of the reaction must be balanced by the cost and practicality of controlling the purity of the substrate on large scale. Consequently, understanding the impact of key impurities can greatly influence the reliability of the RCM reaction.

The RCM transformation depicted in Scheme 1, utilized in the synthesis of SB-462795, a potent cathepsin K inhibitor under

Scheme 1. Synthesis of SB-462795 via the RCM disconnection



development for the treatment of osteoporosis and osteoarthritis,³ clearly exemplifies this point. The formation of the tetrahydroazepine ring in **2** is effected by RCM of diene **1** using Hoveyda's second-generation catalyst⁴ in toluene. With pure diene **1**, this RCM reaction can be performed with very low loadings (0.1–0.2 mol %) of the catalyst; however, the reaction conversion suffers when **1** is of reduced purity. Therefore, significant effort was directed at identifying the impurities which reduced conversion and at controlling their content in **1** in order to afford a robust RCM reaction.

Results and Discussion

Synthesis of Diene 1. The synthesis of diene **1** is detailed in Scheme 2.⁵ Tosylate **3** is converted to epoxide **4** in toluene using DBU as base, and excess DBU is neutralized with aqueous citric acid. After aqueous washes and a solvent

* To whom correspondence should be addressed. Tel: 610-270-5362. Fax: 610-270-4022. E-mail: huan.2.wang@gsk.com.

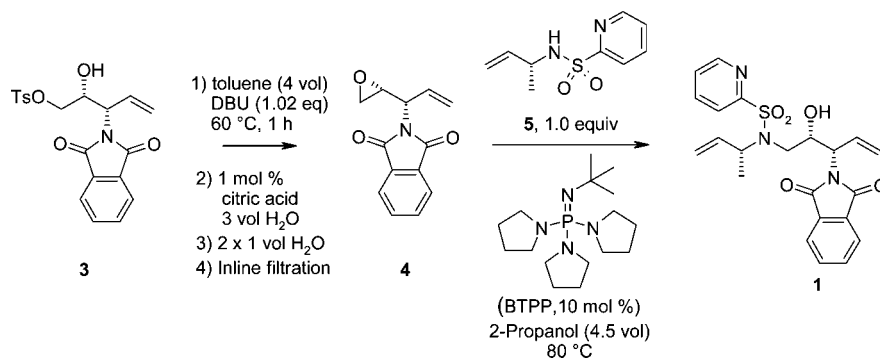
[†] Chemical Development, GlaxoSmithKline.

[‡] Statistical Sciences, GlaxoSmithKline.

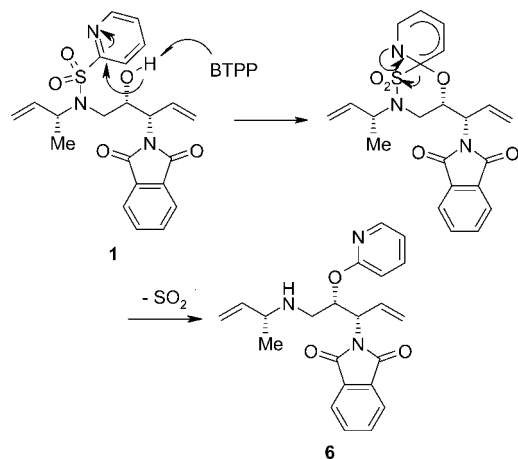
- (1) For general reviews on ring-closing metathesis: (a) Hoveyda, A. H.; Zhugralin, A. R. *Nature* **2007**, *450*, 243. (b) Schrock, R. R. *Angew. Chem., Int. Ed.* **2006**, *45*, 3748. (c) Grubbs, R. H. *Angew. Chem., Int. Ed.* **2006**, *45*, 3760. (d) Grubbs, R. H. *Handbook of Metathesis*; Wiley: Weinheim, 2003 and references cited therein.
- (2) (a) Yee, N. K.; Farina, V.; Houppis, I. N.; Haddad, N.; Frutos, R. P.; Gallou, F.; Wang, X.-j.; Wei, X.; Simpson, R. D.; Feng, X.; Fuchs, V.; Xu, Y.; Tan, J.; Zhang, L.; Xu, J.; Smith-Keenan, L. L.; Vitous, J.; Ridges, M. D.; Spinelli, E. M.; Johnson, M.; Donsbach, K.; Nicola, T.; Brenner, M.; Winter, E.; Kreye, P.; Samstag, W. *J. Org. Chem.* **2006**, *71*, 7133. (b) Nicola, T.; Brenner, M.; Donsbach, K.; Kreye, P. *Org. Process Res. Dev.* **2005**, *9*, 513.

- (3) (a) Kumar, S.; Dare, L.; Vasko-Moser, J. A.; James, I. E.; Blake, S. M.; Rickard, D. J.; Hwang, S.-M.; Tomaszek, T.; Yamashita, D. S.; Marquis, R. W.; Oh, H.; Jeong, J. U.; Veber, D. F.; Gowen, M.; Lark, M. W.; Stroup, G. *Bone* **2007**, *40*, 122. (b) Yamashita, D. S.; Marquis, R. W.; Xie, R.; Nidamarthy, S. D.; Oh, H.-J.; Jeong, J. U.; Erhard, K. F.; Ward, K.W.; Roethke, T. J.; Smith, B. R.; Cheng, H.-Y.; Geng, X.; Lin, F.; Offen, P. H.; Wang, B.; Nevins, N.; Head, M. S.; Haltiwanger, R. C.; Narducci Sarjeant, A. A.; Liable-Sands, L. M.; Zhao, B.; Smith, W. W.; Janson, C. A.; Gao, E.; Tomaszek, T.; McQueney, M.; James, I. E.; Gress, C. J.; Zembryki, D. L.; Lark, M. W.; Veber, D. F. *J. Med. Chem.* **2006**, *49*, 1597. (c) Cummings, M. D.; Marquis, R. W.; Ru, Y.; Thompson, S. K.; Veber, D. F.; Yamashita, D. S. PCT Int. Appl. WO 2001070232 A1, 2001.
- (4) Garber, S. B.; Kingsbury, J. S.; Gray, B. L.; Hoveyda, A. H. *J. Am. Chem. Soc.* **2000**, *122*, 8168.
- (5) The synthesis of tosylate **3** and sulfonamide **5**, as well as a discussion of BTTP-catalyzed epoxide ring-openings, will be disclosed in separate publications.

Scheme 2. Synthesis of diene 1



Scheme 3. Formation of secondary amine 6



exchange from toluene to 2-propanol, epoxide **4** is coupled with sulfonamide **5** in 2-propanol in the presence of a catalytic amount of phosphazene base P1-*tert*-butyl-tris-(tetramethylene) (BTTP). The reaction is complete in 3–5 h with 90–91% crude peak area ratio (PAR) of **1** by HPLC. Aqueous citric acid is then added to solubilize BTTP in the aqueous solution, and a cooled, seeded crystallization delivers the desired product diene **1** in 80% yield.

The formation of the desired product **1** was accompanied by the generation of secondary amine **6**, which increased to 3–5% over prolonged reaction times. This was especially true when high amounts of BTTP were used at high temperatures. Presumably, as the reaction progressed and the concentration of sulfonamide **5** decreased, deprotonation of the product hydroxyl by BTTP became a competitive side reaction. The resultant alkoxide could attack the pyridine ring, leading to irreversible loss of SO₂ and pyridyl migration to the carbinol (Scheme 3).

Design of experiments (DoE)⁶ was used to assess the relationship between the reaction conditions and the reaction profile of the coupling between **4** and **5**. The resultant model indicated that increased concentration would permit lower BTTP loading and minimize formation of **6**, which was verified by scale-up of these conditions to multigram scales. This procedure was used to prepare over 20 batches of **1** which all showed

high levels of purity by HPLC (>98% PAR). However, despite extensive efforts to optimize the process conditions and consistently prepare the product with high purity, different batches of diene **1** thus prepared gave extremely inconsistent results in the subsequent RCM reaction, with conversions ranging from 2% to 100%. The capricious RCM performance of diene **1** prompted a series of detailed studies to identify the impurities responsible for this variability.

Identification of Impurities that Negatively Impact RCM.

Spiking Experiments. In order to identify the impurities that negatively impacted the RCM reaction, an extensive series of spiking experiments was conducted. All known compounds which were a part of the diene preparation, either as input reagent, solvent, or byproduct, were charged in substoichiometric amounts to individual RCM reactions using a batch of diene **1** that gave complete conversion in RCM with 0.2 mol % catalyst. Highlighted results from these studies are summarized in Scheme 4.

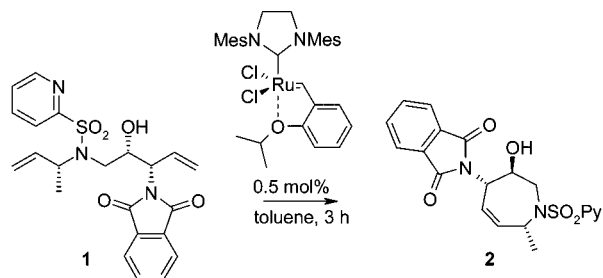
While many suspected agents had no impact on the metathesis of **1**, five impurities were shown to significantly retard the RCM process. Not surprisingly, these impurities all contain either a basic functionality (BTTP, DBU, and secondary amine **6**) or a chelating structure (urea **8** and 2-propyl ester **9**, vide infra). It is worth noting that secondary amine **6** and 2-propyl ester **9** also underwent RCM themselves under the reaction conditions, albeit with much lower efficiency: in the presence of 5 mol % of Hoveyda's catalyst in reflux toluene, the RCM of amine **6** and ester **9** reached 14% and 53% conversion, respectively. More interestingly, urea **8** did not undergo RCM when exposed to Hoveyda's catalyst, even though the reaction between the two seemed facile as 2-isopropoxystyrene was readily generated. Presumably, the urea carbonyl in the resultant alkylidene complex preferentially chelated to the metal center and inhibited the coordination of a second olefin as well as the ring closure. An attempt to isolate this alkylidene complex, however, was not met with success.

Statistical Analysis of Batches. With five possible culprits identified from spiking experiments, it was necessary to determine the extent to which these impurities were present in different batches of **1**. The impurity levels in each batch⁷ are tabulated with its corresponding performance in the RCM reaction, and a graphical depiction of representative data is shown in Figure 1. Although spiking experiments showed that

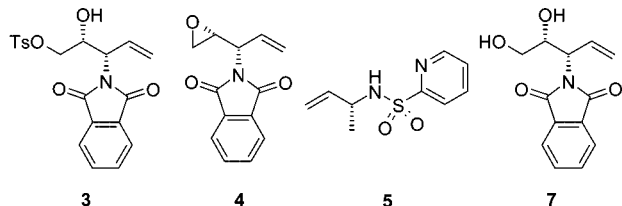
(6) For detailed discussion on DoE methodologies, see: (a) Box, G. E. P.; Hunter, J. S.; Hunter, W. G. *Statistics for Experimenters: Design, Innovation and Discovery*, 2nd ed.; Wiley: New York, 2005. (b) Anderson, M. J.; Whitcomb, P. J. *DoE Simplified: Practical Tools for Effective Experimentation*; Productivity: OR, 2000.

(7) Due to the large difference in UV response for these impurities, all laboratory batches of diene **1** were analyzed using LC-MS, and impurity contents were calculated using calibrated mass signals.

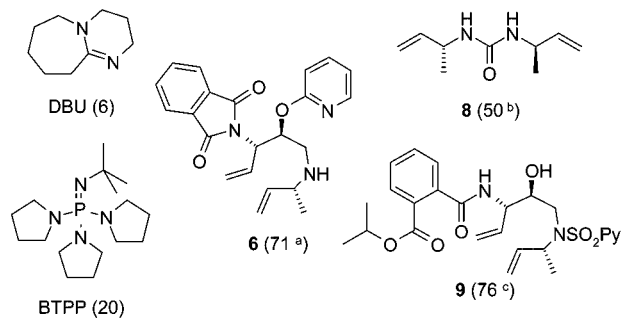
Scheme 4. Spiking studies: Effect of impurities on RCM conversion



Example of impurities which did not effect RCM (> 99% conversion)



Impurities which retarded RCM (RCM conversion/%)



^a Average of four runs; ^b Average of two runs; ^c 0.2 mol% catalyst was used.

DBU negatively impacted the RCM reaction, it was never detected in any of the batches and is therefore omitted from the graph.

In order to identify the impurities that caused the most batch-to-batch variation, the highly correlated data set was analyzed by two projection methods: principal component analysis (PCA) and projection to latent structure (PLS).⁸ PCA transforms complex data sets onto simpler coordinates called principal components. By this method, two principal components were identified which accounted for 99% of the variation in the impurity content in different batches of diene **1**. The score plot in Figure 2a compares the different batches (labeled with batch numbers) in the new coordinate system, with “score” being the coordinates of these batches on the two principal components (t_1 and t_2). Since points close to the origin represent low total impurity levels and all four impurities retard RCM, it is not surprising that only the batches close to the origin gave high conversion in RCM (>80% conversion in RCM with 0.2 mol % catalyst, coded green) while the batches farther from the origin performed poorly (<80% conversion, coded red).

On the other hand, the loading plot in Figure 2b showed the makeup of the two principal components to illustrate how the originally measured impurity levels “loaded into” the two principal components. The higher loading (p) an impurity has,

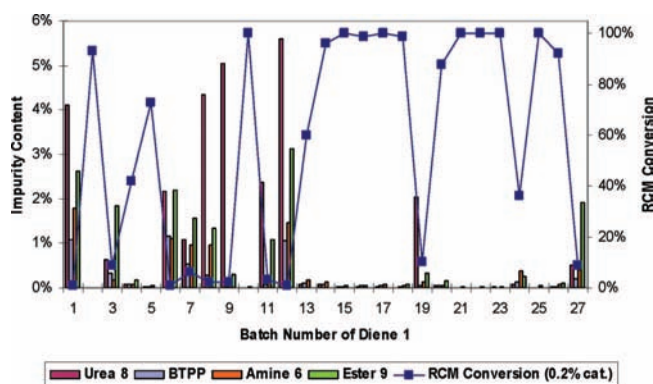


Figure 1. Correlation of impurity content of **1** and performance in the RCM reaction (0.2 mol % catalyst).

the stronger impact it has on that principal component. For instance, urea **8** and ester **9** have the largest p_1 values, indicating that their amounts have the largest influence on the first principal component (t_1). Similarly, the second principal component t_2 is mainly influenced by the amounts of urea **8** and 2-propyl ester **9** as well. Even without any correlation to RCM performance, this indicated that urea **8** and 2-propyl ester **9** accounted for most of the batch-to-batch variation in purity and the content level of these two impurities needed to be controlled and reduced.

While PCA only implicates potential sources of variation in starting material purity, PLS further correlates this variation to the conversion of **1** in the RCM reaction by building a multivariate model between the two. The coefficients of the model are then translated back to the originally measured impurity levels to indicate the magnitude of impact from each on RCM conversion.

The PLS model contains two principal components. As is expected, the first principal component (Figure 3a) shows that all four impurities have negative effects on the RCM conversion, indicating that the overall purity of the starting material is of utmost importance to the reaction conversion. After the first principal component, the dominant influence of urea **8** and 2-propyl ester **9** is again shown by their large negative coefficients in the second principal component (Figure 3b). It suggests that these two impurities negatively impact the RCM performance of **1** even after the overall purity of the starting material has been taken into consideration, thus again implicating them as the two most detrimental impurities.

The PCA and PLS models not only show that impurities **8** and **9** account for the largest source of variation in the starting material quality, they also confirm a strong negative correlation between their content level and RCM performance. This historical data analysis alone does not prove a causal relationship, and neither method of analysis overcomes the issue that the data are heavily correlated. However, the fact that they both arrived at the same conclusion, which was also consistent with the spiking study findings, did provide confidence that focusing our efforts on controlling these two impurities would provide substantial benefit.

Removal of Urea **8, 2-Propyl Ester **9** and Improved Diene Preparation.** *Removal of Urea **8**.* Urea **8** is a known impurity found in almost all batches of sulfonamide **5**, which is prepared by the coupling of 2-pyridinesulfonyl chloride (**10**) with

(8) For detailed discussion of projection methods and their applications, see: *Multi- and Megavariate Data Analysis*; Umetrics: Umea, Sweden, 2006.

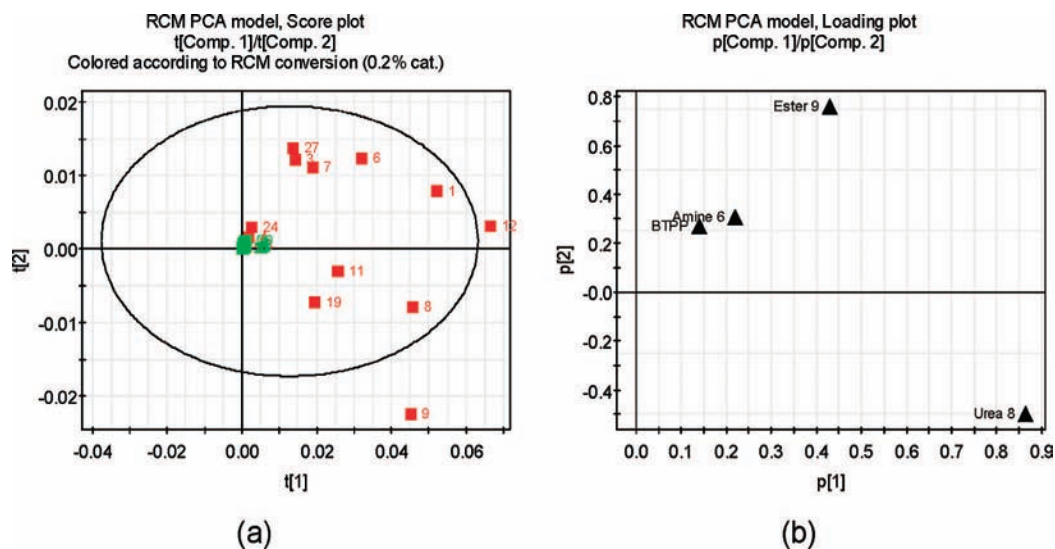


Figure 2. PCA analysis of impurity profile of all batches ($R^2_X = 0.99$, $Q^2_{cum} = 0.88$): (a) the score plot; and (b) the loading plot.

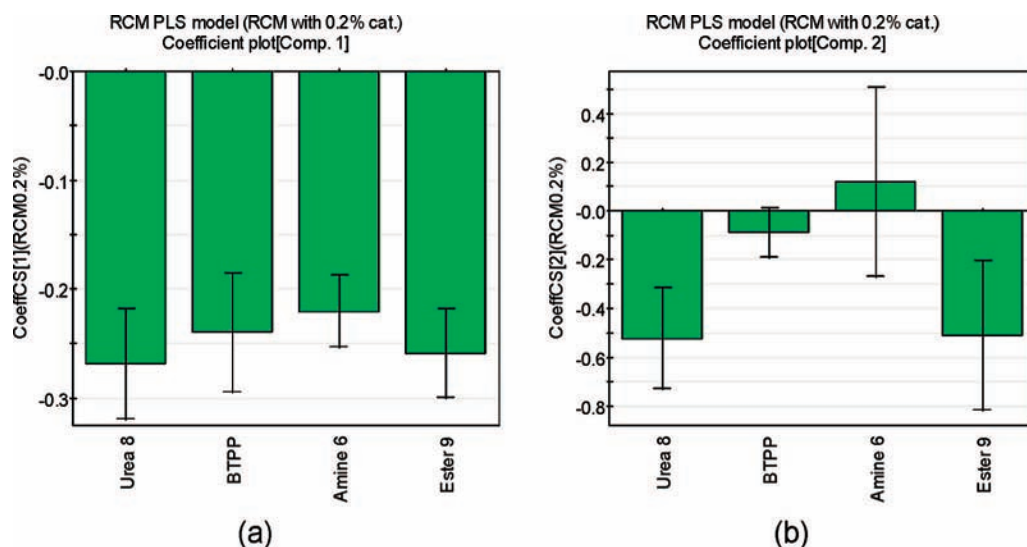
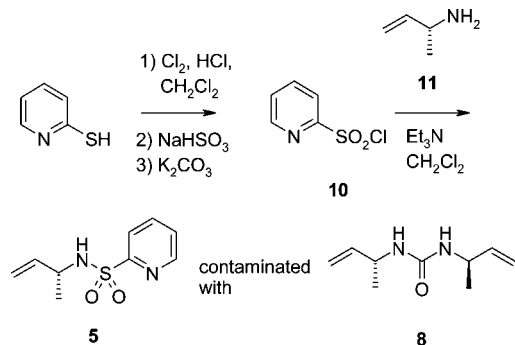


Figure 3. PLS model correlation of impurity content with RCM conversion at 0.2 mol % catalyst ($R^2_X = 0.927$, $R^2_Y = 0.905$, $Q^2_{cum} = 0.854$): coefficient plots of (a) first principal component; and (b) second principal component.

Scheme 5. Preparation of sulfonamide 5



methallylamine **11** (Scheme 5). Historically, the amount of **8** in sulfonamide **5** was observed to be <1% by HPLC, although calibration using a pure standard of urea **8** indicated that some batches of **5** contained as much as 5–7 wt% of this impurity.

It was postulated that a potential source of the one-carbon unit in urea **8** was carbon dioxide, which formed during the aqueous K_2CO_3 wash after the chlorination reaction, remained solubilized in the CH_2Cl_2 solution of **10** and therefore was

present in the reaction mixture during the coupling.⁹ This hypothesis was supported by the observation that only a trace amount of urea **8** was detected in the reaction mixture when the CH_2Cl_2 solution of sulfonyl chloride **10** was concentrated under vacuum prior to the coupling with **11** (Table 1, entry 1), whereas 4 mol % of **8** was observed when the coupling was carried out using the CH_2Cl_2 solution of **10** directly after the K_2CO_3 wash (entry 2). Carbon dioxide was further implicated as the carbon source of urea **8** by the observed formation of a large amount of **8** when dry ice was added to a mixture of amine **11** and Et_3N prior to the addition of sulfonyl chloride **10** in the coupling reaction (entry 3). One plausible mechanism illustrating the role of CO_2 in the formation of **8** is depicted in Scheme 6.

With the likely origin of **8** identified, the problem was easily solved by replacing K_2CO_3 with NaOH in the chlorination

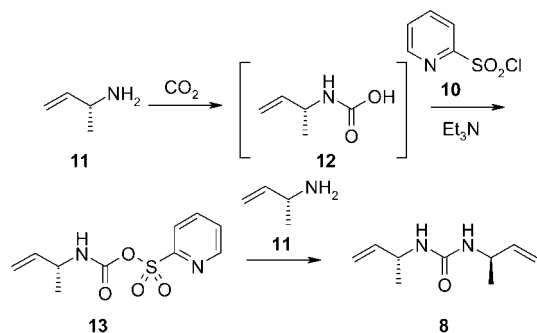
(9) It was also postulated that co-solvent CH_2Cl_2 could form phosgene (or a phosgene equivalent) during the oxidation of mercaptopyridine, which would then be trapped by amine **11** during the subsequent coupling step to form urea **8**. However, this proposal was invalidated as urea **8** was observed in sulfonamide **5** even when the chlorination was conducted in solvents such as toluene or chlorotoluene.

Table 1. Quantities of urea 8 formed under different reaction conditions

entry	form of 10 used in coupling	additive	urea 8 /mol%
1	oil ^a	—	0.05
2	solution ^b	—	4
3	oil ^a	CO ₂ (s)	27

^a After aq K₂CO₃ workup, sulfonyl chloride **10** was concentrated to an oil prior to coupling with amine **11**. ^b After aq K₂CO₃ workup, sulfonyl chloride **10** was used directly as a CH₂Cl₂ solution in the coupling.

Scheme 6. Possible mechanism for the formation of 8 with CO₂



workup. The sulfonyl chloride solution thus obtained produced only a trace amount of urea **8** in the coupling reaction mixture, and no urea was detected in the isolated solid of sulfonamide **5**.

The acidity of sulfonamide **5** also allowed it to be readily deprotonated by alkaline solutions and represented a convenient handle for its purification. Thus, sulfonamide **5** (contaminated with urea **8**) was treated with aqueous NaOH to furnish an aqueous solution of its sodium salt, leaving solid urea **8** to be filtered off. Sulfonamide **5** was recovered after simple reacidification with HCl. This procedure allowed us to rework large quantities of contaminated material, affording pure sulfonamide **5** which contained undetectable quantities of the urea impurity.

Removal of 2-Propyl Ester 9. 2-Propanol adduct **9** was identified relatively late during development work. In fact, it was hardly detectable in early laboratory batches of diene **1**. Unfortunately, it became a significant problem during a 1.5 kg scale-up experiment, at which point it was produced in ~2.2 mol %.¹⁰

Interestingly, 2-propyl ester **9** was not observed in solution during the coupling reaction between sulfonamide **5** and epoxide **4**, but only formed after the quench with aqueous citric acid. Since a neutral water quench still led to the formation of appreciable quantities of **9**, a nonaqueous workup was investigated. The acid quench was initially included to protonate the BTPP catalyst and prevent it from oiling out when the product precipitated. However, the discovery that BTPP was miscible with heptane led to the development of an anhydrous isolation using heptane as the antisolvent. Using the modified procedure, pure product containing very low levels of BTPP and no significant quantities of 2-propyl ester **9** was routinely obtained.

Improved Diene Preparation. Having identified the two main impurities and methods for their removal, the synthesis of the

diene was optimized for throughput, yield and process efficiency. The reaction was carried out with urea-free sulfonamide **5**. Upon completion of the reaction, a seeded cooling crystallization using heptane as the antisolvent then provided an easily filterable slurry, producing large, uniform crystals with low cake resistance upon filtration. Figure 4 illustrates that the product isolated by this method (Figure 4b) appears to be more consistent in size and aspect ratio in relation to the previous isolation procedure, which used an aqueous citric acid quench and did not control particle formation (Figure 4a). The diene thus prepared was of consistently high purity, typically containing only negligible amounts of BTPP and secondary amine **6**, and no urea **8** or 2-propyl ester **9**.

RCM Performance of Representative Batch and Specification Setting. *RCM Performance of Representative Batch.* With the procedure for diene **1** finalized and representative batches available, the RCM procedure was optimized using Response Surface Methodology (RSM).¹¹ A central composite design with temperature (60–90 °C), reaction volume (5–10 volumes) and catalyst loading (0.1–0.3 mol %) revealed that reaction volume had no impact on the reaction.¹² The conversion was determined by reaction temperature and catalyst loading, with complete RCM achieved at high temperature and high catalyst loading (Figure 5a). The experimental space where the reaction would reach complete conversion is indicated by the yellow region in the overlay plot (Figure 5b).

The model also provided a basis for assessing the robustness of the reaction. Although the long-term consistency of the RCM reaction cannot be demonstrated by a limited number of experiments, the probability of its achieving a desired conversion can be assessed using a Bayesian reliability approach based on the RSM model data.¹³ Therefore, a probability function was established for reaching specific conversions at a given catalyst loading and reaction temperature. The probability of achieving complete RCM conversion (>95%) and, thus, the robustness of the process under different reaction conditions were then calculated for each catalyst loading/temperature combination across the experimental region (Figure 6). At low temperature and/or low catalyst loading, the probability of complete RCM conversion is very low, as indicated by the green color coding. The probability rises with higher catalyst loading and higher temperature, with the calculated 50% probability contour almost identical to the edge of the yellow region in the overlay plot in Figure 5b, which corresponds to the predicted mean of RCM conversion. With high temperature and sufficient catalyst loading, over 90% probability can be reached within this experimental space. Therefore, a catalyst loading of 0.25 mol % and a temperature of 80 °C were selected as the final reaction conditions for the RCM, with a calculated probability of >95% for achieving complete RCM conversion.

Specification Setting. Another aspect of robustness is tolerance of the reaction of impurities in the starting material.

(11) For detailed discussion on RSM and their applications, see: Anderson, M. J.; Whitcomb, P. J. *RSM Simplified: Optimizing Processes Using Response Surface Methods for Design of Experiments*; Productivity: New York, 2005.

(12) No cross-metathesis product was observed even when the reaction was run at the highest concentration.

(13) (a) Peterson, J. J. *J. Qual. Technol.* **2004**, *36*, 139. (b) Miro-Quesada, G.; Del Castillo, E.; Peterson, J. J. *J. Appl. Stat.* **2004**, *31*, 291.

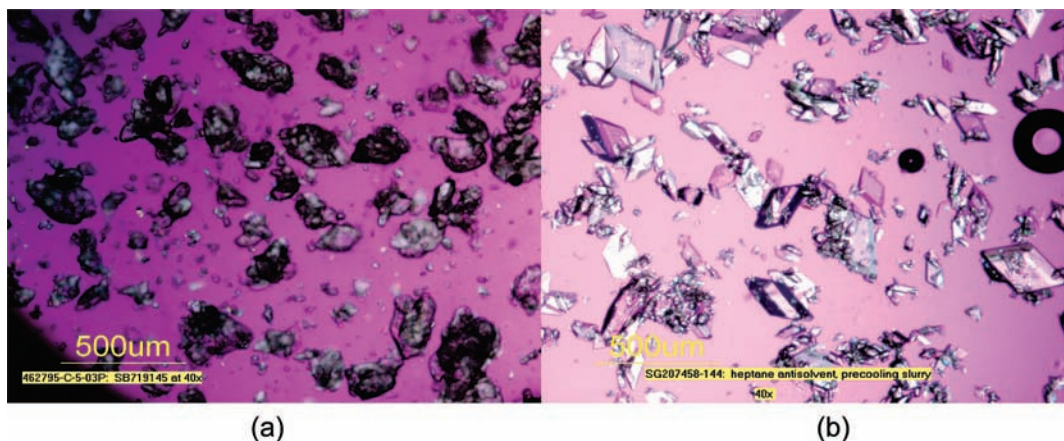


Figure 4. Comparison of product crystals: material isolated from the citric acid procedure (a) versus material produced using a controlled crystallization with heptane as antisolvent (b).

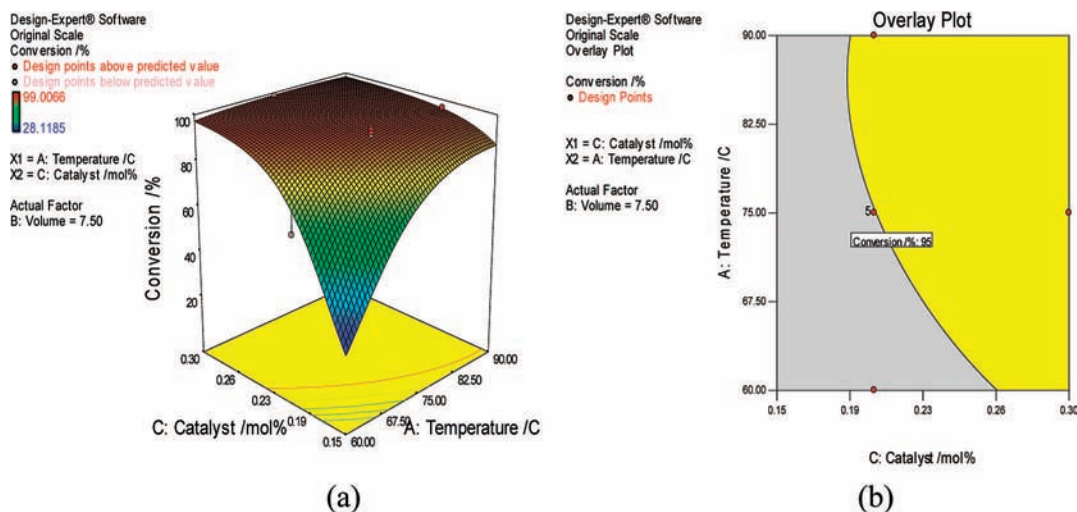


Figure 5. (a) Response surface model and (b) overlay plot of RCM conversion.

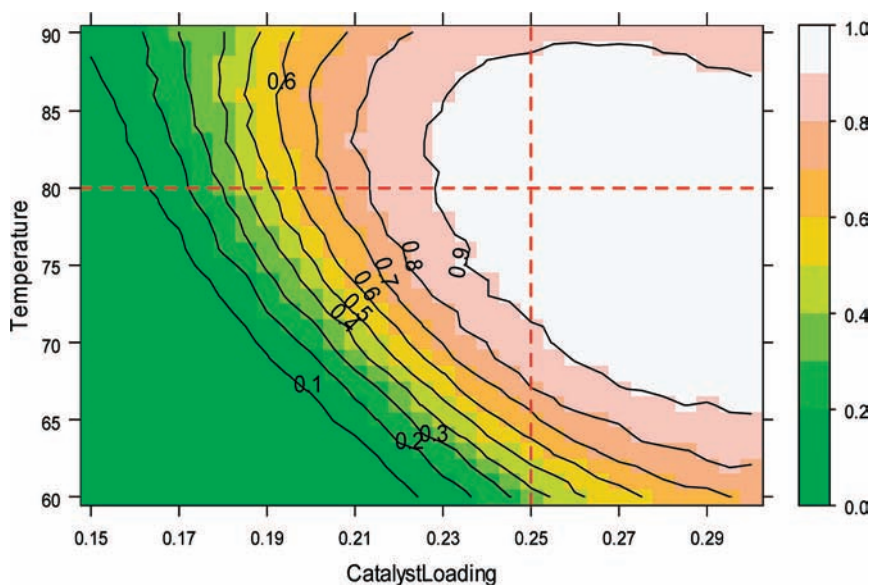


Figure 6. Probability of reaching complete conversion in RCM using a representative batch of 1.

Although historical data were available (vide supra), they could not be used to set univariate specifications due to the heavy correlation in the data. An orthogonal design had to be used for this purpose, and the robustness of the specifications could

then be assessed by model-based probability of a successful RCM reaction using this material.

Therefore, a two-level factorial DoE was performed where different amounts of the four main impurities (urea **8**: 0–0.05

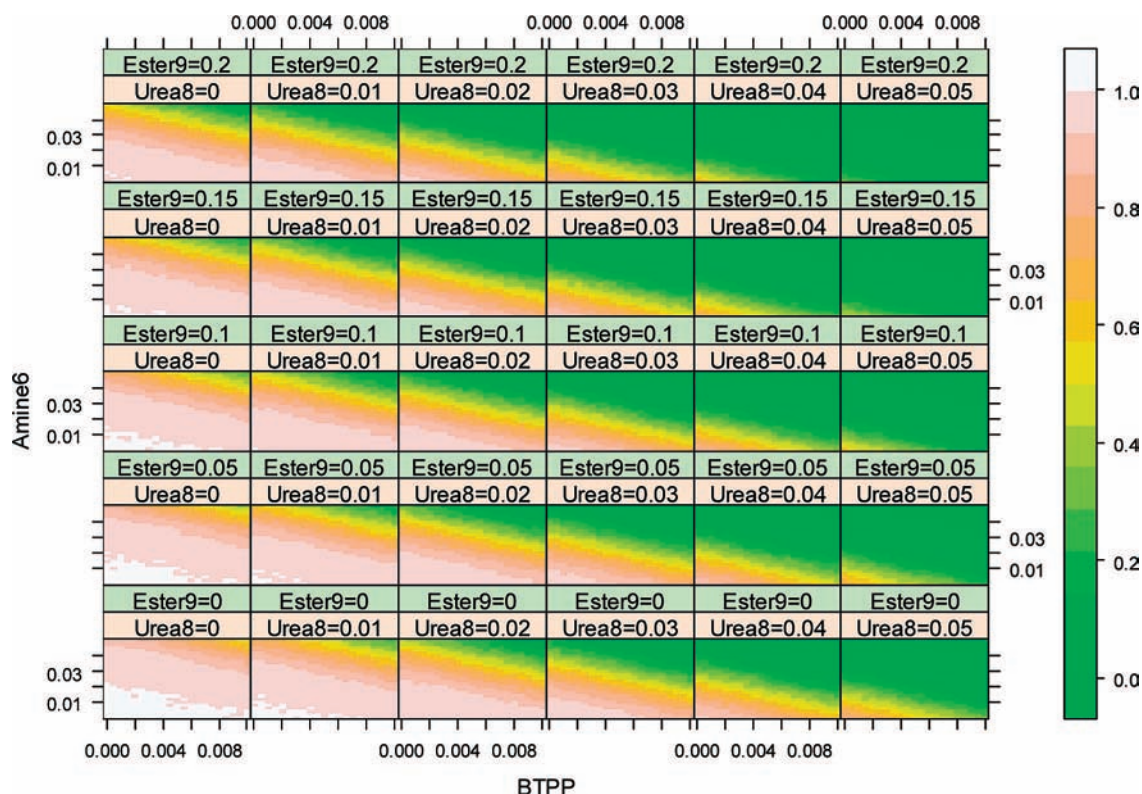


Figure 7. Probability of achieving complete RCM using diene **1** with different purity profile.

mol %; BTTP: 0–0.01 mol %; amine **6**: 0–0.05 mol %; 2-propyl ester **9**: 0–0.2 mol %) were spiked into a representative batch of **1**.¹⁴ The RCM reaction was then carried out under the standard conditions and the reaction conversion was modelled against the impurity levels. Consistent with findings from spiking experiments and PLS interpretations, all four impurities showed a statistically significant, negative impact on the RCM conversion.

Again with an empirical model available, the probability of complete RCM conversion was calculated for different levels of impurity contents in the starting material. The reliability plot is shown in Figure 7: The probability of achieving complete conversion is very high (~100%) with the unspiked batch (the panel at the lower left corner), but decreases with higher amounts of spiked impurities. When all four impurities were spiked (the upper right corner in the figure), the probability of reaching complete conversion is essentially zero. Based on the calculated probability results, specifications of the four impurities could then be set: Urea **8** <0.01 mol %, BTTP <0.007 mol %, amine **6** <0.01 mol % and 2-propyl ester **9** <0.15 mol %.¹⁵ Under the standard RCM conditions, a batch of **1** containing all four impurities at these levels would have >90% probability of reaching completion in the RCM reaction.

Scale-Up Results of the RCM Reaction. With robustness of the RCM reaction significantly increased from improved starting material purity and optimized reaction conditions, scale-up of the reaction was conducted. Using diene prepared by the modified procedure under optimized RCM conditions, the

reaction consistently gave >99% conversion in 20–50 g jacketed laboratory reactor experiments. Scale-up of the reaction culminated in a plant run, where the reaction was carried out on a 6.7 kg scale. With 0.25 mol % catalyst loading, the reaction proceeded smoothly in five volumes of toluene, reaching completion within two hours at 80 °C. A simple cool-down and filtration then afforded the cyclized product in 90% yield, with a residual ruthenium content of 121 ppm.¹⁶

Conclusion

The development of a robust and high-yielding synthesis of **2** using RCM is described. The work is highlighted by: (1) spiking studies to identify individual impurities which negatively affect the RCM reaction; (2) historical data analysis using projection methods to identify the main sources of variation in starting material quality and determine the main detrimental impurities in starting material, which led to (3) subsequent modification of the starting material synthesis to ensure diene **1** of high purity, which in turn ensured a robust RCM process; and (4) a probability-based approach in response surface optimization and reaction robustness assessment.

Experimental Section

General. Unless otherwise indicated, all reactions were conducted under a nitrogen atmosphere. Solvents and reagents

(14) Impurity content in this batch: urea **8**: not detected; BTTP: 0.006 mol %; amine **6**: 0.03 mol %; 2-propyl ester **9**: not detected.

(15) Including the impurities in the starting material, the specifications should be: urea **8**: <0.01 mol %; BTTP: <0.013 mol %; amine **6**: <0.04 mol %; 2-propyl ester **9**: <0.15 mol %.

(16) The residual ruthenium was effectively purged through the subsequent four chemical transformations and the final particle formation, with all intermediates being solids and isolated through crystallization. RCM product **2** with as much as 427 ppm of Ru has been used in multikilo campaigns and no ruthenium (<1 ppm) was detected in any batches of the final API. Most of the purging is believed to occur during the hydrogenation of **2**, where Ru can be adsorbed by the charcoal support of Pd/C catalyst. On laboratory scale, hydrogenated product with less than 1 ppm of Ru was obtained from a batch of **2** that contained 359 ppm of Ru.

were obtained from commercial sources and used without further purification. Hoveyda's catalyst was purchased from Materia Inc. in Pasadena, California. All DoE data were processed using Design-Expert Version 7.0.3, PCA and PLS models were analyzed using SIMCA-P+ 11, reliability calculations were carried out in SAS 9.1.

1,3,4,5-Tetradecoxy-3-(1,3-dioxo-1,3-dihydro-2H-isoindol-2-yl)-1-[(1R)-1-methyl-2-propen-1-yl]amino]-2-O-2-pyridinyl-L-threo-pent-4-enitol (6). Diene **1** (1.0 g, 2.27 mmol) and Cs₂CO₃ (0.775 g, 2.38 mmol) were heated in acetonitrile (5 mL) to 80 °C and stirred overnight. Upon cooling, the slurry was filtered through celite to remove solid residues, and the solvent removed under vacuum. The product was purified by flash column chromatography: 0.60 g, 70% yield. ES-MS: *m/z*: 378 (M + H⁺). ¹H NMR (CDCl₃, 300 MHz) δ 7.88 (ddd, 1H, *J* = 5.0, 2.1, 0.8 Hz), 7.70 (m, 2H), 7.63 (m, 2H), 7.33 (ddd, 1H, *J* = 9.1, 7.1, 2.0 Hz), 6.61 (ddd, 1H, *J* = 7.2, 5.0, 0.9 Hz), 6.54 (dm, 2H, *J* = 9.2 Hz), 6.45 (m, 1H), 6.05 (m, 1H), 5.67 (m, 1H), 5.48 (dm, 1H, *J* = 17 Hz), 5.32 (dd, 1H, *J* = 9.8, 1.4 Hz), 5.16 (t, 1H, *J* = 9.4 Hz), 5.01 (m, 2H), 3.13 (m, 2H), 2.81 (dd, 1H, *J* = 13, 6.2 Hz), 1.13 (d, 3H, *J* = 6.5 Hz). ¹³C NMR (CDCl₃, 100 MHz) δ 167.83, 163.11, 146.53, 142.64, 138.44, 133.53, 131.83, 131.69, 122.83, 120.73, 116.71, 114.10, 111.01, 72.99, 56.47, 56.41, 47.87, 21.32.

N,N'-Bis[(1R)-1-methyl-2-propen-1-yl]urea (8). [(1R)-1-Methyl-2-propen-1-yl]amine hydrochloride (4.0 g, 37.4 mmol) was stirred in acetonitrile (24 mL) at room temperature. To this slurry was added triethylamine (5.73 mL, 41.1 mmol), then CDI (3.64 g, 22.4 mmol). After stirring the slurry overnight, the solvent was removed under vacuum, and the residue partitioned between EtOAc and water. Upon separation of the layers, the organic layer was washed sequentially with sat. aq. NH₄Cl, sat. aq. NaHCO₃, brine, then dried over Na₂SO₄. The desiccant was filtered and solvent removed under vacuum to provide a slightly yellow solid (4 g). Pure **8** was obtained by treating the crude solid with hot TBME (25–30 mL), diluting with hexanes, cooling slowly to 5 °C and filtering on a Buchner funnel: 2.376 g, 76% yield. ES-MS: *m/z*: 169 (M + H⁺). ¹H NMR (CDCl₃, 300 MHz) δ 5.84 (m, 2H), 5.04–5.20 (m, 4H), 4.29 (m, 2H), 1.22 (dd, 6H, *J* = 6.8, 4.3 Hz). ¹³C NMR (CDCl₃, 100 MHz) δ 157.63, 140.86, 113.21, 47.39, 20.93.

1,3,4,5-Tetradecoxy-3-[(2-[(1-methylethyl)oxy]carbonyl)phenyl]carbonylamino]-1-[(1R)-1-methyl-2-propen-1-yl](2-pyridinylsulfonyl)amino]-L-threo-pent-4-enitol (9). Diene **1** (2.99 g, 6.77 mmol) was suspended in EtOH (20 mL) and N₂H₄ hydrate (1.0 mL, 20.6 mmol, 3.0 equiv) was added at room temperature. The mixture turned clear within a few minutes. It was stirred at room temperature overnight and turned into a white suspension. NaOH (1 N, 20 mL) was added and the mixture was extracted with CH₂Cl₂ (20 mL × 2). The organic layer was dried and concentrated. The crude aminoalcohol was dissolved in CH₂Cl₂ (20 mL). Isopropyl hydrogen phthalate¹⁷ (1.48 g, 7.11 mmol, 1.05 equiv), EDCI (1.50 g, 7.82 mmol, 1.16 equiv) and HOObt (57.7 mg, 0.354 mmol, 0.05 equiv) were added at 0 °C. The mixture was stirred at 0 °C for 3 h and diluted with HCl (1 N, 20 mL). The layers were separated, and the aqueous layer was extracted with CH₂Cl₂ (20 mL). The

combined organic layer was dried and concentrated. The product was purified by flash column chromatography: 2.67 g, 5.32 mmol, 79% yield. ES-MS: *m/z*: 502 (M + H⁺), 524 (M+Na⁺). ¹H NMR (CDCl₃, 300 MHz) δ 8.66 (dm, 1H, *J* = 4.8 Hz), 8.08 (dt, 1H, *J* = 7.9, 1.0 Hz), 7.95 (td, 1H, *J* = 7.7, 1.7 Hz), 7.89 (dm, 1H, *J* = 7.8 Hz), 7.52 (m, 4H), 6.43 (d, 1H, *J* = 9.1 Hz), 6.05 (m, 1H), 5.81 (m, 1H), 5.47 (dm, 1H, *J* = 17, 1.4 Hz), 5.32 (dt, 1H, *J* = 10.4, 1.4 Hz), 5.23 (dd, 1H, *J* = 12.5, 6.3 Hz), 5.05 (d, 1H, *J* = 1.5 Hz), 5.02 (dm, 1H, *J* = 6.6 Hz), 4.72 (m, 1H), 4.28 (m, 2H), 3.79 (dd, 1H, *J* = 15.2, 10.4 Hz), 3.56 (dd, 1H, *J* = 15.2, 2.7 Hz), 1.34 (d, 9H, *J* = 6.2 Hz). ¹³C NMR (CDCl₃, 100 MHz) δ 169.02, 165.86, 157.97, 149.41, 138.64, 138.09, 137.12, 136.45, 131.53, 130.16, 129.87, 129.54, 127.37, 126.94, 123.25, 117.16, 116.05, 71.29, 68.92, 55.73, 52.99, 48.10, 21.76, 21.59, 17.59.

General Procedure for Spiking Experiments. In a vial, diene **1** (100–200 mg) and Hoveyda's catalyst (0.5 mol %) were dissolved in toluene (1–2 mL) under nitrogen, and the impurity (0.5–0.8 mol %) was added to the reaction mixture. The resultant solution was heated to reflux for 3–5 h and the reaction conversion was determined by HPLC.

1,3,4,5-Tetradecoxy-3-(1,3-dioxo-1,3-dihydro-2H-isoindol-2-yl)-1-[(1R)-1-methyl-2-propen-1-yl](2-pyridinylsulfonyl)amino]-L-threo-pent-4-enitol (1). In a glass-lined reactor, a slurry of tosylate **3** (8.5 kg, 21.2 mol) and toluene (34 L) was heated to 56 °C under nitrogen, and DBU (3.3 kg, 21.7 mol) was added via pressure vessel to maintain the temperature between 55 and 65 °C. The starting material dissolved during the addition and the mixture was aged at this temperature for 60 min. Upon completion of the reaction, the mixture was cooled to 25 °C and 10% w/w aq. citric acid (0.42 L water with 45 g citric acid monohydrate) was added. After stirring for 10 min, water (25.5 L) was added, the mixture stirred and the layers allowed to separate. The organic layer was then washed twice with water (2 × 8.5 L). The solution of crude **4** was then transferred to a second reactor via an inline filter to remove a small layer of film, and the transfer line then rinsed with toluene (8.5 L). To this second reactor was charged **5** (4.5 kg, 21.2 mol) and the solvent partially removed by vacuum distillation to reach 15 L total volume (36.0 L toluene removed). 2-Propanol (25.5 L) was charged and the system vacuum distilled to achieve 15 L total volume (25.5 L removed). The total solvent volume was adjusted to 3.4 volumes using 2-propanol (15.0 L added), BTTP (0.7 kg, 2.12 mol) was added and the mixture heated to 80 °C over ~30 min. After aging for 3.5 h, the reaction was complete, and heptane was added (17.0 L) while maintaining the temperature ≥60 °C. The temperature was then adjusted to 53 °C and seeds of **1** (4.5 g in 2:1 heptane:2-propanol) were charged to the reactor. The slurry was held at 52 °C for 60 min, then cooled to ~10 °C at 0.5 °C/min. After holding for 30 min, the slurry was isolated by centrifugal filtration, washed with cold heptane/2-propanol (2:1 v/v, 2 × 8.5 L). The product was dried under vacuum at 45 °C to afford **1**: 7.25 kg (16.4 mol, 78%), >99.9% pure by HPLC. ¹H NMR (CDCl₃, 400 MHz) δ 8.62 (dm, 1H, *J* = 4.0 Hz), 8.02 (d, 1H, *J* = 7.9 Hz), 7.93 (td, 1H, *J* = 7.7, 1.6 Hz), 7.83 (m, 2H), 7.70 (m, 2H), 7.50 (dm, 1H, *J* = 0.9 Hz), 6.29 (m, 1H), 5.81 (m, 1H), 5.39 (d, 1H, *J* = 17.1 Hz), 5.30 (dd, 1H, *J* = 10.2, 0.5 Hz), 5.13 (m, 2H), 4.89 (bs,

(17) Loev, B.; Kormendy, M. *J. Org. Chem.* **1962**, *27*, 1703.

1H), 4.68 (t, 1H, $J = 9.0$ Hz), 4.60 (dt, 1H, $J = 9.2, 2.6$ Hz), 4.39 (m, 1H), 3.56 (dd, 1H, $J = 15.1, 2.6$ Hz), 3.45 (dd, 1H, $J = 15.3, 9.2$ Hz), 1.30 (d, 3H, $J = 6.9$ Hz). ^{13}C NMR (CDCl_3 , 100 MHz) δ 168.6, 158.6, 150.1, 138.9, 137.9, 134.3, 132.7, 132.4, 127.2, 123.7, 123.4, 121.3, 117.7, 69.2, 58.1, 56.2, 49.4, 18.1.

2-[(3*S*,4*S*,7*R*)-3-Hydroxy-7-methyl-1-(2-pyridinylsulfonyl)-2,3,4,7-tetrahydro-1*H*-azepin-4-yl]-1*H*-isoindole-1,3(2*H*)-dione (**2**). In a glass-lined reactor, diene **1** (6.74 kg, 15.3 mol) and Hoveyda's catalyst (24 g, 0.038 mol, 0.25 mol %) were dissolved in toluene (34 L), and the mixture was sparged with nitrogen (3.4 L/min) for 1 h. With continued nitrogen sparging, the mixture was heated first to 60 °C over 20 min, then to 80 °C over 45 min. The reaction mixture was stirred at 80 °C for 2 h, and HPLC showed the reaction was complete. The mixture was heated to 92 °C and the nitrogen sparging was discontinued. The reaction mixture was cooled to 5 °C over 3 h and held at 5 °C overnight. The product was collected by centrifugal filtration, rinsed with cold toluene (13.5 L), and dried under vacuum at 50 °C: 5.70 kg (13.8 mol, 90%), 99.45% purity by HPLC PAR. Ru content: 121 ppm. ^1H NMR (CDCl_3 , 400 MHz) δ 8.81 (dm, 1H, $J = 4.0$ Hz), 8.05 (d, 1H, $J = 7.8$ Hz), 7.97

(td, 1H, $J = 7.8, 1.6$ Hz), 7.75 (m, 2H), 7.66 (m, 2H), 7.60 (m, 1H), 5.52 (m, 1H), 5.20 (m, 2H), 5.02 (br, 1H), 4.63 (m, 1H), 4.42 (dd, 1H, $J = 9.6, 4.4$ Hz), 4.21 (d, 1H, $J = 16$ Hz), 3.87 (dd, 1H, $J = 16, 4.6$ Hz), 1.31 (d, 3H, $J = 6.9$ Hz). ^{13}C NMR (CDCl_3 , 100 MHz) δ 19.65, 48.29, 52.77, 54.75, 71.54, 122.29, 123.01, 126.68, 126.76, 130.95, 131.60, 133.85, 138.62, 150.62, 157.20, 168.01.

Acknowledgment

We thank Dr. Hayao Matsuhashi and Ms. Jessica Bailey for their initial efforts in developing this chemistry, Mr. Christopher Werner for his contributions to the robust crystallization of **1**, Dr. Grant Spoor for helpful discussion in the mechanism of urea formation, Mr. Tom Wrzosek for helpful discussion in PCA/PLS modeling, and Dr. John Peterson for discussion in the application of Bayesian predictive approach to process optimization.

Received for review December 14, 2007.

OP700288P